

ExoMol line lists – XLI. High-temperature molecular line lists for the alkali metal hydroxides KOH and NaOH

A. Owens,^{*} J. Tennyson[†] and S. N. Yurchenko[‡]

Department of Physics and Astronomy, University College London, Gower Street, WC1E 6BT London, UK

Accepted XXXX. Received XXXX; in original form XXXX

ABSTRACT

Potassium hydroxide (KOH) and sodium hydroxide (NaOH) are expected to occur in the atmospheres of hot rocky super-Earth exoplanets but a lack of spectroscopic data is hampering their potential detection. Using robust first-principles methodologies, comprehensive molecular line lists for KOH and NaOH that are applicable for temperatures up to $T = 3500$ K are presented. The KOH OYT4 line list covers the $0–6000$ cm^{-1} (wavelengths $\lambda > 1.67$ μm) range and comprises 38 billion transitions between 7.3 million energy levels with rotational excitation up to $J = 255$. The NaOH OYT5 line list covers the $0–9000$ cm^{-1} (wavelengths $\lambda > 1.11$ μm) range and contains almost 50 billion lines involving 7.9 million molecular states with rotational excitation up to $J = 206$. The OYT4 and OYT5 line lists are available from the ExoMol database at www.exomol.com and should greatly aid the study of hot rocky exoplanets.

Key words: molecular data – opacity – planets and satellites: atmospheres – stars: atmospheres – ISM: molecules.

1 INTRODUCTION

Simple molecules composed of rock-forming elements, such as potassium hydroxide (KOH) and sodium hydroxide (NaOH), are expected to be present in the atmospheres of hot rocky super-Earth exoplanets (Schaefer et al. 2012; Tennyson & Yurchenko 2017a). This class of exoplanets are in close proximity to their host star and tidally-locked, with their dayside exposed to extremely high temperatures, e.g. up to 4000 K. The material on the surface of the planet will vaporise to create an atmosphere strongly dependent on the initial planetary composition (Schaefer & Fegley 2009; Miguel et al. 2011). Probing the spectroscopy of hot rocky super-Earths poses its own unique set of challenges, notably the availability of molecular line lists for relevant molecules composed of rock-forming elements, and the completeness of these line lists at such high temperatures.

The possible detection of KOH and NaOH in exoplanets could help identify terrestrial planets with molten surfaces (Hamano et al. 2013), and lead to a better understanding of the relationship between the atmosphere and crust of hot rocky exoplanets at high temperatures ($\gtrsim 3500$ K) (Herbort et al. 2020). However, only a small amount of spectroscopic data is available for the alkali metal hydroxides KOH and NaOH, which are linear triatomic molecules in the gas phase. The Cologne Database for Molecular Spectroscopy (CDMS) (Müller et al. 2001; Müller et al. 2005) lists a number of pure rotational transitions in the microwave region for KOH and NaOH as they are considered to be interstellar molecules, despite only the tentative identification of NaOH in the molecular cloud Sagittarius B2 (Hollis & Rhodes 1982) and star-forming region Orion-KL (Turner 1991). Aside from the CDMS data, which is based on several laboratory measurements of these molecules (Pearson et al. 1976; Kuijpers et al. 1975; Raw et al. 1987; Kawashima et al. 1996; Cederberg et al. 1996; Pearson & Trueblood 1973; Kuijpers et al. 1976; Kawashima et al. 1996), there is a lack of reliable rotation-vibration information for KOH and NaOH. Previous studies have tried to establish the fundamental vibrational wavenumbers but the situation is unclear with some debate in the literature and differing values presented (discussed further in Section 3.3). Thus, the process of generating molecular line lists for KOH and NaOH is far more reliant on theory, particularly the quantum chemical methods used to build the spectroscopic model of the molecule, i.e. the potential energy and dipole moment surfaces. These first-principles methodologies (Tennyson 2016; Tennyson & Yurchenko 2017b) are routinely employed by the ExoMol project (Tennyson & Yurchenko 2012) and enable the computation of line lists containing many billions of molecular transitions (Tennyson et al. 2016, 2020). Importantly, these methods can enable the production of complete line lists suitable for elevated temperatures. Already a large number of diatomic

^{*} The corresponding author: alec.owens.13@ucl.ac.uk

[†] The corresponding author: j.tennyson@ucl.ac.uk

[‡] The corresponding author: s.yurchenko@ucl.ac.uk

and polyatomic species have been treated within the ExoMol framework (Tennyson & Yurchenko 2018), with many line lists relevant to the spectroscopy of hot rocky super-Earths.

In this paper, we present comprehensive molecular line lists for KOH and NaOH that are suitable for modelling exoplanet and other hot atmospheres with temperatures up to 3500 K. The line lists have been generated using robust first-principles calculations based on newly computed, high-level *ab initio* potential energy and dipole moment surfaces. Work similar in spirit was recently carried out on another hot rocky super-Earth molecule, silicon dioxide (SiO₂) (Owens et al. 2020), resulting in a line list containing nearly 33 billion transitions between 5.69 million rotation-vibration states with rotational excitation up to $J = 255$, where J is the total angular momentum quantum number of the molecule.

2 METHODS

A full description of the computational approach used to generate the molecular line lists of KOH and NaOH is provided in the supplementary material and only a brief summary is given here. The methodology is very similar to our previous work on silicon dioxide (Owens et al. 2020). To begin with, high-level electronic structure methods were employed to construct the potential energy surface (PES) and electric dipole moment surface (DMS) of each molecule in its ground electronic state. Particular emphasis was placed on the accuracy of the *ab initio* methods used to compute the PESs, as there is very little experimental data on these molecules and the PESs would not be empirically refined. Generally speaking, with the chosen *ab initio* methods, the PES of KOH can be expected to reproduce the fundamental term values to within 3–5 cm⁻¹, while the PES of NaOH to within 1–3 cm⁻¹ as conservative estimates (e.g. see Owens et al. (2018) and references within). Transition intensities computed using *ab initio* DMSs are comparable to, if not occasionally more reliable, than experiment (Yurchenko 2014; Tennyson 2014), and for KOH and NaOH we expect them to be within 5–10% of experimentally determined intensities.

All surfaces were computed on extensive grids of nuclear geometries (tens of thousands of points) with energies up to $hc \cdot 30\,000$ cm⁻¹ (h is the Planck constant and c is the speed of light). The *ab initio* data was then fitted with appropriate three-dimensional analytic representations and incorporated into variational calculations with the nuclear motion code TROVE (Yurchenko et al. 2007). Line list calculations for KOH and NaOH were very similar and followed standard TROVE procedures, notably taking advantage of a new linear triatomic molecule implementation (Yurchenko & Mellor 2020) that was recently used to compute high-temperature line lists for silicon dioxide (Owens et al. 2020) and carbon dioxide (Yurchenko et al. 2020). Rovibrational calculations utilised a large symmetry-adapted basis set with testing to ensure convergence of the $J = 0$ vibrational states. Note that the potential energy and dipole moment surfaces are provided as supplementary material along with Fortran routines to construct them.

The KOH OYT4 line list was computed with a lower state energy threshold of $hc \cdot 16\,000$ cm⁻¹ (h is the Planck constant and c is the speed of light) and considered transitions up to $J = 255$ in the 0–6000 cm⁻¹ range. A total of 38 362 078 911 transitions between 7 307 923 energy levels were computed for the OYT4 line list. For the NaOH OYT5 line list, a lower state energy threshold of $hc \cdot 16\,000$ cm⁻¹ was used with transitions considered up to $J = 206$ in the 0–9000 cm⁻¹ range. A total of 49 663 923 0921 transitions between 7 927 877 energy levels were computed for the OYT5 line list. Figures showing the distribution of transitions and energy levels of each line list as a function of J are shown in the supplementary material. In both molecules, the largest number of computed transitions and states occurs before $J = 30$ and then steadily decreases as a result of an upper state energy threshold in the line list calculations.

Commenting on the quantum numbers and molecular symmetry of KOH and NaOH, the rovibrational energy levels and wavefunctions of both molecules were classified under the $C_s(M)$ molecular symmetry group (Bunker & Jensen 1998) where the nuclear spin statistical weights are $g_{\text{ns}} = \{8, 8\}$ for states of symmetry $\{A', A''\}$, respectively. Transitions follow the symmetry selection rules $A' \leftrightarrow A''$; and the standard rotational selection rules, $J' - J'' = 0, \pm 1$, $J' + J'' \neq 0$; where $'$ and $''$ denote the upper and lower state, respectively. Traditionally, the vibrational and rotational modes of asymmetric linear molecules are classified according to irreducible representations of $C_{\infty v}(M)$: Σ^+/Σ^- , Π , Δ etc. The overall rovibrational wavefunctions can only be of Σ^+ or Σ^- symmetry (see, e.g. Bunker & Jensen (1998)), which correlate to $C_s(M)$ as $A' \leftrightarrow \Sigma^+$ and $A'' \leftrightarrow \Sigma^-$. Another standard spectroscopic descriptor is the Kronig parity e/f (Brown et al. 1975), related to the total parity $+1$ (A') and -1 (A'') as follows: the parity of the e state is $(-1)^J$ while the parity of the f state is $(-1)^{J+1}$. The vibrational quantum numbers used by TROVE (discussed further in the supplementary material) were correlated to the following standard spectroscopic quantum numbers used for linear-type triatomic molecules: $v_1, v_2^{\text{lin}}, L = |l|, v_3$, where v_1 and v_3 are the stretching quantum numbers, v_2^{lin} is the bending quantum number used for linear molecules and l is the corresponding vibrational quantum number. The two bending quantum numbers v_2^{lin} and l are related to the ‘non-linear’ bending quantum number v_2 by $v_2^{\text{lin}} = 2v_2 + l$ with $L = v_2^{\text{lin}}, v_2^{\text{lin}} - 2, \dots, 0(1)$. The symmetries of the vibrational and rotational contributions span the A' and A'' irreducible representations in $C_s(M)$ and $\Sigma^{+/-}$ ($L = 0$), Π ($L = 1$), Δ ($L = 2$) etc. in $C_{\infty v}$. The rotational quantum number k_a is constrained to the vibrational angular momentum by $k_a = l$.

Table 1. Extract from the `.states` file of the KOH OYT4 line list.

i	\tilde{E}	g_{tot}	J	unc	Γ_{tot}	v_1	v_2^{lin}	L	v_3	C_i	n_1	n_2	n_3
1	0.000000	8	0	4.000000	A'	0	0	0	0	1.00	0	0	0
2	441.302845	8	0	4.000000	A'	1	0	0	0	1.00	1	0	0
3	655.924321	8	0	8.000000	A'	0	2	0	0	1.00	0	0	1
4	877.113398	8	0	8.000000	A'	2	0	0	0	1.00	2	0	0
5	1081.543317	8	0	12.000000	A'	1	2	0	0	1.00	1	0	1
6	1269.577195	8	0	16.000000	A'	0	4	0	0	1.00	0	0	2
7	1307.451689	8	0	12.000000	A'	3	0	0	0	1.00	3	0	0
8	1501.902919	8	0	16.000000	A'	2	2	0	0	1.00	2	0	1
9	1687.220972	8	0	20.000000	A'	1	4	0	0	1.00	1	0	2
10	1732.331589	8	0	16.000000	A'	4	0	0	0	1.00	4	0	0

i : State counting number;
 \tilde{E} : Term value (in cm^{-1});
 g_{tot} : Total state degeneracy;
 J : Total angular momentum quantum number;
unc: Estimated uncertainty of energy level (in cm^{-1});
 Γ_{tot} : Overall symmetry in $C_s(M)$ (A' or A'');
 $v_1, v_2^{\text{lin}}, L, v_3$: Linear-molecule vibrational quantum numbers;
 C_i : Largest coefficient used in the TROVE assignment;
 n_1, n_2, n_3 : TROVE vibrational quantum numbers.

Table 2. Extract from the `.trans` file for the $0-100\text{ cm}^{-1}$ window of the KOH OYT4 line list.

f	i	A_{if}
2997983	3068742	5.87023848E-05
656704	579657	2.18505406E-02
832462	859993	7.59010951E-06
1583619	1610495	1.26488417E-04
243548	225006	7.77221741E-10
3760055	3692577	4.66414104E-03
4615110	4673426	1.49445735E-05
582879	607777	1.20942018E-04
5072485	5090674	2.24346842E-05
5391819	5376327	4.14086508E-05

f : Upper state ID; i : Lower state ID;
 A_{if} : Einstein A coefficient (in s^{-1}).

3 RESULTS

3.1 Line list format

As standard, the OYT4 and OYT5 line lists are provided in the ExoMol data format. The most up-to-date information on the ExoMol data format can be found in the recent ExoMol 2020 database release paper (Tennyson et al. 2020). Further information can also be found in the ExoMol 2016 database release paper (Tennyson et al. 2016) if needed. In short, the `.states` file, see Table 1 for an example of the KOH OYT4 `.states` file (identical structure for the NaOH OYT5 line list), contains all the computed rovibrational energy levels (in cm^{-1}), each labelled with a unique state ID counting number, symmetry and quantum number labelling, and the contribution C_i from the largest eigencoefficient used to assign the rovibrational state. The `.trans` files contain all the computed transitions with upper and lower state ID labels and Einstein A coefficients, see Table 2 for an example of the KOH OYT4 `.trans` file (identical structure for the NaOH OYT5 line list), and have been separated into 100 cm^{-1} frequency bins for user-handling purposes. In addition to the complete OYT4 and OYT5 line lists, which contain tens of billions of lines, more compact versions of these line lists, e.g. using the super-lines format, will be made available on the ExoMol website (www.exomol.com) in due course.

3.2 Temperature-dependent partition functions

The temperature-dependent partition function $Q(T)$, defined as

$$Q(T) = \sum_i g_i \exp\left(\frac{-E_i}{kT}\right), \quad (1)$$

where $g_i = g_{\text{ns}}(2J_i + 1)$ is the degeneracy of a state i with energy E_i and rotational quantum number J_i , has been calculated for KOH and NaOH by summing over all computed rovibrational energy levels on a 1 K grid in the 1–4000 K range (provided

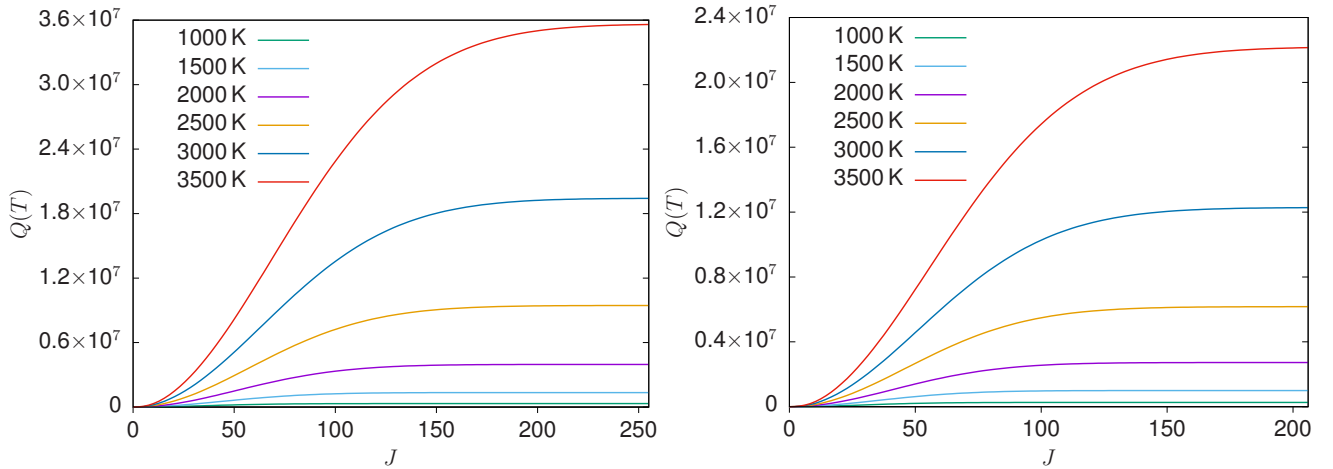


Figure 1. Convergence of the partition function $Q(T)$ of KOH (left panel) and NaOH (right panel) with respect to the rotational quantum number J at different temperatures.

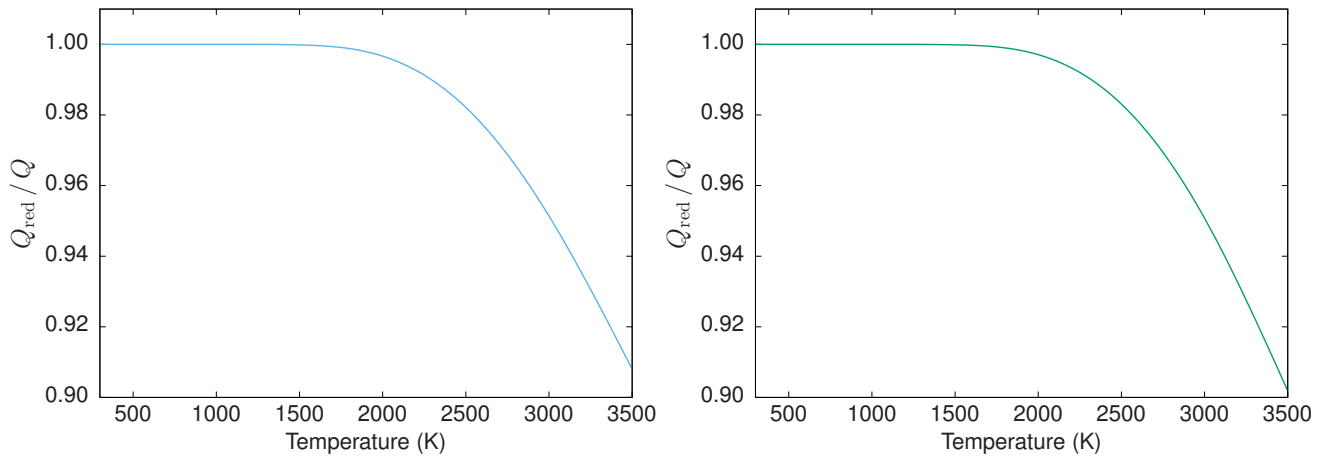


Figure 2. The ratio Q_{red}/Q as a function of temperature T for KOH (left panel) and NaOH (right panel); this gives a measure of the completeness of the line lists.

as supplementary material). The convergence of $Q(T)$ as a function of J for different temperatures is shown in Fig. 1. As expected, the partition function converges quickly at lower temperatures but this changes dramatically for temperatures above 2500 K, where a significant number of higher J states must be considered in the summation of Eq. (1). At $J = 255$, the value of $Q(3500 \text{ K})$ is converged to 0.007% for KOH, while for NaOH the value of $Q(3500 \text{ K})$ at $J = 206$ is converged to 0.012%.

Both the KOH and NaOH line lists were computed with a lower state energy threshold of $hc \cdot 16\,000 \text{ cm}^{-1}$. To gain insight into the completeness of these line lists it is informative to calculate the reduced partition function $Q_{\text{red}}(T)$, which only includes energy levels up to $hc \cdot 16\,000 \text{ cm}^{-1}$ in the summation of Eq. (1). In Fig. 2, the ratio $Q_{\text{red}}(T)/Q(T)$ has been plotted with respect to temperature for KOH (left panel) and NaOH (right panel). At lower temperatures $Q_{\text{red}}/Q = 1.00$, indicating completeness of the line list as the partition function values are not altered by the lower state energy threshold. Above 1500 K the ratio starts to decrease from unity and by 3500 K the ratio $Q_{\text{red}}/Q \approx 0.90$. This should be regarded as a soft temperature limit for the OYT4 and OYT5 line lists. Any use of these line lists above this temperature may result in a progressive loss of opacity, however, the missing opacity contribution can be estimated from Q_{red}/Q if needed (Neale et al. 1996).

3.3 Simulated spectra of KOH and NaOH

An overview of the spectrum of KOH and NaOH is shown in Fig. 3, where we have simulated integrated absorption cross-sections at a resolution of 1 cm^{-1} , modelled with a Gaussian line profile with a half width at half maximum (HWHM) of 1 cm^{-1} . Spectral simulations were carried out with the EXOCROSS program (Yurchenko et al. 2018b). The line positions of the strongest absorption bands are in close agreement between KOH and NaOH, which is to be expected given their structural similarity. Both molecules possess strong fundamental bands below 1000 cm^{-1} (wavelengths $\lambda > 10 \text{ }\mu\text{m}$) attributed to the ν_2 bending mode at 343 cm^{-1} in KOH and 228 cm^{-1} in NaOH, and the ν_1 stretching mode around 441 cm^{-1} in KOH and

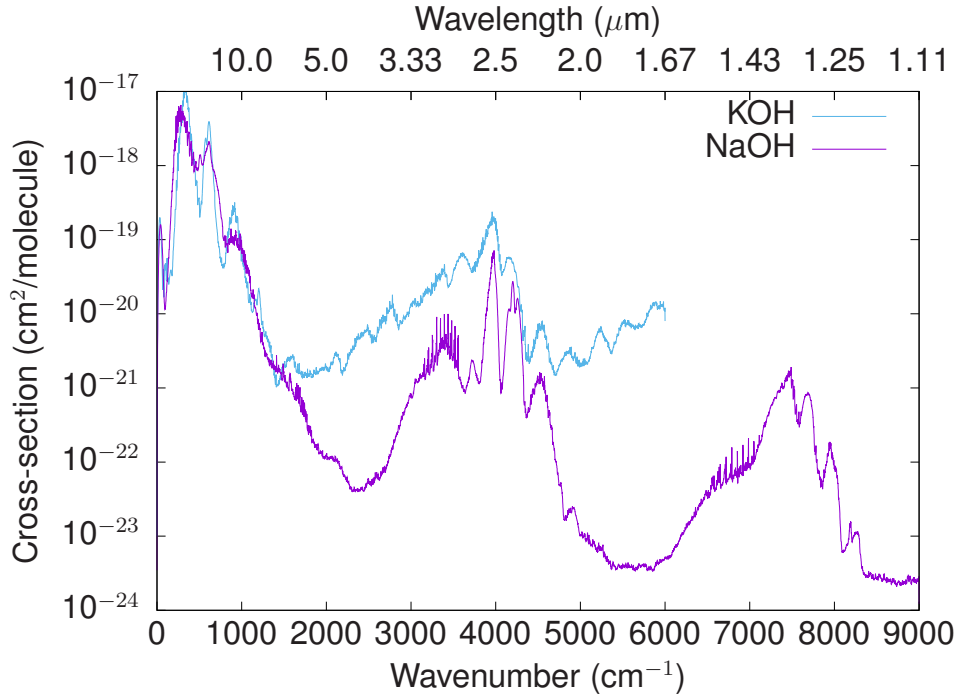


Figure 3. Spectra of KOH and NaOH at $T = 1000$ K. Absorption cross-sections were computed from the OYT4 and OYT5 line lists at a resolution of 1 cm^{-1} and modelled with a Gaussian line profile with a half width at half maximum (HWHM) of 1 cm^{-1} .

562 cm^{-1} in NaOH. The next strongest band in both molecules is due to the fundamental ν_3 O–H stretching mode, occurring around 3735 cm^{-1} in KOH and 3784 cm^{-1} in NaOH.

The values given above for the fundamental wavenumbers have been calculated in this study. In the past, efforts have been made to establish the values of the fundamentals of KOH and NaOH but the situation remains unclear and there has been some debate in the literature with differing values presented. The reader is referred to the section on molecular constants on pages 1046–1050 of [Gurvich et al. \(1997\)](#) for KOH and pages 1261–1263 of [Gurvich et al. \(1996\)](#) for NaOH. These two papers provide a description of previous spectroscopic studies on these molecules and then go on to estimate values for their own work on the calculation of thermal functions. For KOH, these values are: $\nu_1 = 408 \pm 10 \text{ cm}^{-1}$, $\nu_2 = 300 \pm 10 \text{ cm}^{-1}$, $\nu_3 = 3700 \pm 100 \text{ cm}^{-1}$; and for NaOH: $\nu_1 = 540 \pm 20 \text{ cm}^{-1}$, $\nu_2 = 300 \pm 20 \text{ cm}^{-1}$, $\nu_3 = 3700 \pm 100 \text{ cm}^{-1}$. Despite not being in complete agreement with these estimated values, we are confident that our calculated fundamental wavenumbers are in fact closer to the true values based on the *ab initio* theory used in this work to construct the spectroscopic models. For KOH, the fundamental bands should be reliable to within $3\text{--}5 \text{ cm}^{-1}$ and for NaOH to within $1\text{--}3 \text{ cm}^{-1}$ as conservative estimates. We have performed further checks by computing harmonic vibrational frequencies using high-level *ab initio* methods with the quantum chemistry program MOLPRO ([Werner et al. 2012](#)) and the results are consistent with our predictions.

The temperature dependence of the OYT4 and OYT5 line lists is shown in Fig. 4, where absorption cross-sections at a resolution of 1 cm^{-1} using a Gaussian profile with a HWHM of 1 cm^{-1} have been plotted for a variety of temperatures. As the temperature increases the rotational band envelopes are significantly broadened by the increased population of vibrationally excited states and the spectrum becomes smoother and more featureless, particularly in KOH above 1000 cm^{-1} (wavelengths $\lambda < 10 \text{ }\mu\text{m}$).

The Cologne Database for Molecular Spectroscopy (CDMS) ([Müller et al. 2001](#); [Müller et al. 2005](#)) contains a number of pure rotational transitions in the microwave region for these molecules. For KOH, CDMS lists 61 lines up to $J = 61$, determined using an effective Hamiltonian model based on observed microwave transitions from [Pearson et al. \(1976\)](#); [Kuijpers et al. \(1975\)](#); [Raw et al. \(1987\)](#); [Kawashima et al. \(1996\)](#). The CDMS KOH transition intensities are based on an experimentally-determined electric dipole moment value of 7.415 Debye in the ground vibrational state ([Cederberg et al. 1996](#)). Regarding NaOH, there are 72 lines up to $J = 72$ based on measurements from [Pearson & Trueblood \(1973\)](#); [Kuijpers et al. \(1976\)](#); [Kawashima et al. \(1996\)](#) with line intensities derived from a dipole moment value of 6.832 Debye ([Kawashima et al. 1996](#)). Note that we have compared with the hyperfine-unresolved data from CDMS.

In Fig. 5, the KOH OYT4 stick spectrum at $T = 300 \text{ K}$ is plotted against the data from CDMS (left panel). The rotational band is reproduced well, with the OYT4 spectrum exhibiting more structure and lines as it extends up to $J = 255$. The right panel of Fig. 5 shows the residual errors $\Delta\nu(\text{obs} - \text{calc})$ (in cm^{-1}) between the observed CDMS wavenumbers and the computed OYT4 wavenumbers up to $J' = 8$, where J' is the rotational quantum number of the upper state involved in the

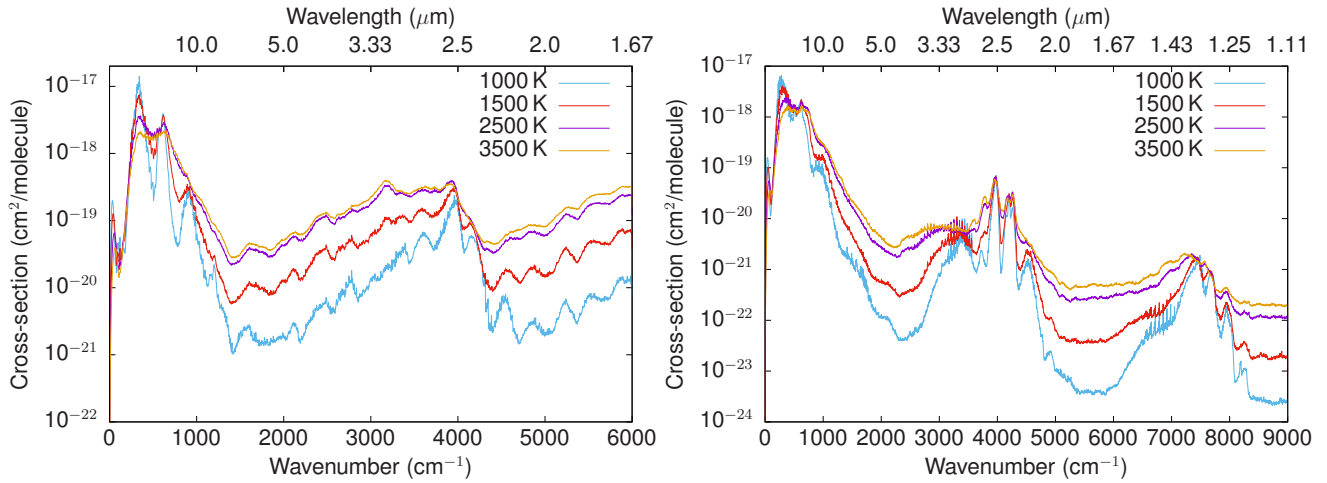


Figure 4. Temperature dependence of the spectrum of KOH (left panel) and NaOH (right panel). Absorption cross-sections were computed from the OYT4 and OYT5 line lists at a resolution of 1 cm^{-1} and modelled with a Gaussian line profile with a half width at half maximum (HWHM) of 1 cm^{-1} .

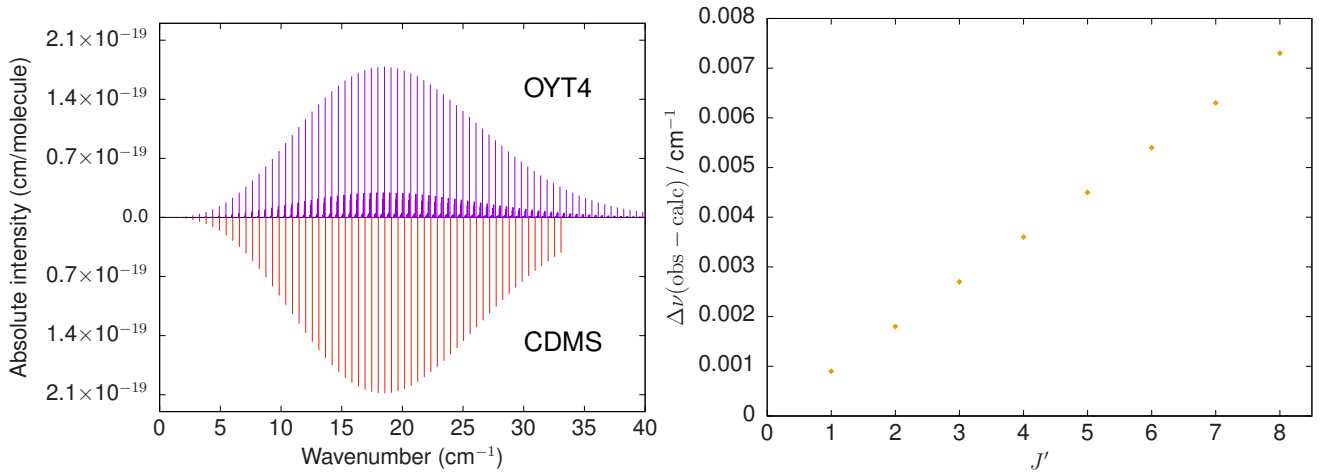


Figure 5. Comparison of the KOH OYT4 line list with CDMS (Müller et al. 2001; Müller et al. 2005). The left panel shows an OYT4 stick spectrum at $T = 300 \text{ K}$ plotted against all transition data from CDMS. The right panel shows the residual errors $\Delta\nu(\text{obs} - \text{calc})$ (in cm^{-1}) between the observed CDMS wavenumbers and the computed OYT4 wavenumbers up to $J' = 8$, where J' is the rotational quantum number of the upper state involved in the pure rotational transition.

pure rotational transition, e.g. $J' = 1$ corresponds to the $1 \leftarrow 0$ line. At each step up in J' , the residual error increases by $\approx 0.001 \text{ cm}^{-1}$. This is a very small error and confirms the quality of our computational approach, notably the accuracy of the *ab initio* PES. Computed OYT4 line intensities are marginally smaller compared to the CDMS values and we are inclined to believe that the OYT4 values are more reliable since they are based on a high-quality *ab initio* DMS and more sophisticated model.

A similar picture is obtained for the NaOH OYT5 line list when compared with the CDMS data, which can be seen in Fig. 6. Rotational band shape is well reproduced with the OYT5 spectrum showing more structure due to the increased coverage up to $J = 206$. Again the residual errors $\Delta\nu(\text{obs} - \text{calc})$ are small and increase by $\approx 0.001 \text{ cm}^{-1}$ for each J' ; a reflection of the quality of the *ab initio* PES. The computed OYT5 line intensities are also weaker than the CDMS values but are still believed to be more reliable. Overall there is good agreement for both KOH and NaOH with the CDMS data.

4 CONCLUSION

Comprehensive molecular line lists have been presented for the alkali metal hydroxides KOH and NaOH. The KOH OYT4 line list covers the $0\text{--}6000 \text{ cm}^{-1}$ range (wavelengths $\lambda > 1.67 \mu\text{m}$) for states below $J = 255$ and is applicable for temperatures up to 3500 K . The NaOH OYT5 line list covers the $0\text{--}9000 \text{ cm}^{-1}$ range (wavelengths $\lambda > 1.11 \mu\text{m}$) for states below $J = 206$ and is also applicable for temperatures up to 3500 K . Both line lists have been constructed using purely *ab initio* methods with no

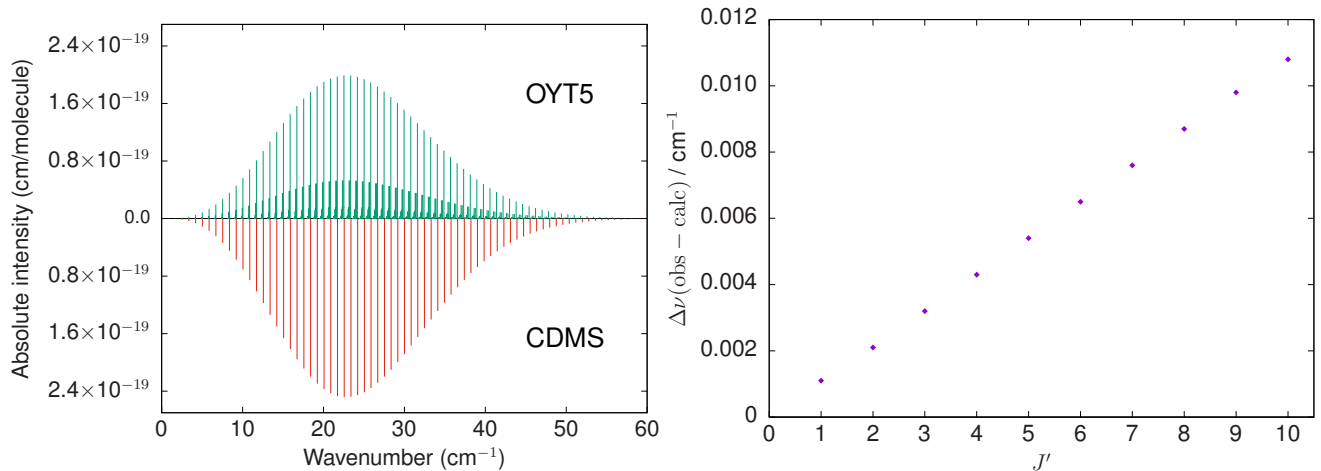


Figure 6. Comparison of the NaOH OYT5 line list with CDMS (Müller et al. 2001; Müller et al. 2005). The left panel shows an OYT5 stick spectrum at $T = 300$ K plotted against all transition data from CDMS. The right panel shows the residual errors $\Delta\nu(\text{obs} - \text{calc})$ (in cm^{-1}) between the observed CDMS wavenumbers and the computed OYT5 wavenumbers up to $J' = 10$, where J' is the rotational quantum number of the upper state involved in the pure rotational transition.

stage of empirical refinement to the spectroscopic model, thus limiting the accuracy of the predicted line positions, particularly for highly excited states and shorter wavelengths. For KOH, the fundamental bands should be reliable to within $3\text{--}5 \text{ cm}^{-1}$ and for NaOH to within $1\text{--}3 \text{ cm}^{-1}$ as conservative estimates. Computed transition intensities are expected to be within $5\text{--}10\%$ of experimentally determined intensities. These are, however, only error estimates based on our previous experience building *ab initio* spectroscopic models with similar electronic structure methods. To truly quantify the accuracy of the presented line lists would require reliable experimental data and we encourage further spectroscopic investigations into these systems. Certainly the comparisons of the OYT4 and OYT5 pure rotational bands with the CDMS data are encouraging and give us confidence in our calculations.

Usually the ExoMol procedure to construct a line list will incorporate a stage of refinement of the spectroscopic model to laboratory data to improve the accuracy of the line list, notably the line positions (Tennyson 2012). Whilst this has not been possible for KOH and NaOH, purely *ab initio* line lists can still be valuable in interpreting astronomical spectra. For example, the original hydrogen cyanide (HCN) / hydrogen isocyanide (HNC) line list of Harris et al. (2002) was computed at a lower level of *ab initio* theory (van Mourik et al. 2001) than that used in the present study. This HCN / HNC line list has underpinned many recent (possible) detections of HCN in exoplanets (Tsiaras et al. 2016; Hawker et al. 2018; Gandhi et al. 2020), having been updated (Harris et al. 2006; Barber et al. 2014), and even adapted to H^{13}CN (Harris et al. 2008), by the *post hoc* insertion of empirical energy levels, a process that is explicitly allowed for by the ExoMol data format (Tennyson et al. 2013). Should high-resolution spectroscopic data become available for KOH and NaOH, a similar update will occur. With that in mind, the OYT4 and OYT5 line lists are only recommended for low-resolution studies of exoplanet atmospheres, e.g. with a resolving power of $R \approx 100$, and are not suitable for high-resolution analysis.

While the extraterrestrial presence of NaOH and KOH largely relies on the predictions of models, the spectrum of another hydroxide, CaOH, is thought to play an important role in the atmospheres of M-dwarf stars (Pesch 1972; Tsuji 1973; Bernath & Brazier 1985; Dick et al. 2006). Indeed, Rajpurohit et al. (2013) studied missing opacity in the BT-Settl cool star model for M-dwarfs which they assigned to the lack of line lists for three species, namely AlH, NaH and CaOH. The ExoMol project has since provided line lists for AlH (Yurchenko et al. 2018a) and NaH (Rivlin et al. 2015) leaving CaOH as the outstanding problem. However, CaOH is a more complicated system than NaOH or KOH since it has an extra, unpaired electron meaning that it is an open shell system with low-lying electronic states. It is these states which provide the CaOH spectral features and opacities in M-dwarfs. While some work has been done on computing rovibronic transition intensities (Zak et al. 2017), so far we have not computed a full rovibronic line list for a triatomic system. Work is currently underway adapting the program EVEREST (Mitrushchenkov 2012), which is designed to treat the Renner-Teller effect in the excited electronic states found in CaOH, for this purpose. A full rovibronic line list for CaOH will be published as part of the ExoMol series in due course.

ACKNOWLEDGMENTS

This work was supported by the STFC Projects No. ST/M001334/1 and ST/R000476/1. The authors acknowledge the use of the UCL Legion High Performance Computing Facility (Legion@UCL) and associated support services in the completion of this work, along with the Cambridge Service for Data Driven Discovery (CSD3), part of which is operated by the University of

Cambridge Research Computing on behalf of the STFC DiRAC HPC Facility (www.dirac.ac.uk). The DiRAC component of CSD3 was funded by BEIS capital funding via STFC capital grants ST/P002307/1 and ST/R002452/1 and STFC operations grant ST/R00689X/1. DiRAC is part of the National e-Infrastructure.

DATA AVAILABILITY

The data underlying this article are available from the ExoMol database at www.exomol.com.

REFERENCES

- Adler T. B., Knizia G., Werner H. J., 2007, *J. Chem. Phys.*, 127, 221106
- Barber R. J., Strange J. K., Hill C., Polyansky O. L., Mellau G. C., Yurchenko S. N., Tennyson J., 2014, *MNRAS*, 437, 1828
- Bernath P. F., Brazier C. R., 1985, *ApJ*, 288, 373
- Brown J. M., et al., 1975, *J. Mol. Spectrosc.*, 55, 500
- Bunker P. R., Jensen P., 1998, *Molecular Symmetry and Spectroscopy*, 2 edn. NRC Research Press, Ottawa
- Carter S., Handy N., Sutcliffe B., 1983, *Mol. Phys.*, 49, 745
- Cederberg J., et al., 1996, *J. Chem. Phys.*, 105, 3361
- Cooley J. W., 1961, *Math. Comp.*, 15, 363
- Császár A. G., Allen W. D., Schaefer III H. F., 1998, *J. Chem. Phys.*, 108, 9751
- Dick M. J., Sheridan P. M., Wang J. G., Yu S., Bernath P. F., 2006, *J. Mol. Spectrosc.*, 240, 238
- Douglas M., Kroll N. M., 1974, *Ann. Phys.*, 82, 89
- Dunning T. H., 1989, *J. Chem. Phys.*, 90, 1007
- Gandhi S., et al., 2020, *MNRAS*, 495, 224–237
- Gurvich L. V., Bergman G. A., Gorokhov L. N., Iorish V. S., Leonidov V. Y., Yungman V. S., 1996, *J. Phys. Chem. Ref. Data*, 25, 1211
- Gurvich L. V., Bergman G. A., Gorokhov L. N., Iorish V. S., Leonidov V. Y., Yungman V. S., 1997, *J. Phys. Chem. Ref. Data*, 26, 1031
- Hamano K., Abe Y., Genda H., 2013, *Nature*, 497, 607
- Harris G. J., Polyansky O. L., Tennyson J., 2002, *ApJ*, 578, 657
- Harris G. J., Tennyson J., Kaminsky B. M., Pavlenko Y. V., Jones H. R. A., 2006, *MNRAS*, 367, 400
- Harris G. J., Larner F. C., Tennyson J., Kaminsky B. M., Pavlenko Y. V., Jones H. R. A., 2008, *MNRAS*, 390, 143
- Hättig C., 2005, *Phys. Chem. Chem. Phys.*, 7, 59
- Hawker G. A., Madhusudhan N., Cabot S. H. C., Gandhi S., 2018, *ApJL*, 863, L11
- Herbort O., Woitke P., Helling C., Zerkle A., 2020, *A&A*, 636, A71
- Heß B. A., 1986, *Phys. Rev. A*, 33, 3742
- Hill J. G., Peterson K. A., 2010, *Phys. Chem. Chem. Phys.*, 12, 10460
- Hill J. G., Peterson K. A., 2017, *J. Chem. Phys.*, 147, 244106
- Hill J. G., Peterson K. A., Knizia G., Werner H.-J., 2009, *J. Chem. Phys.*, 131, 194105
- Hill J. G., Mazumder S., Peterson K. A., 2010, *J. Chem. Phys.*, 132, 054108
- Hollis J. M., Rhodes P. J., 1982, *ApJ*, 262, L1
- Jørgensen U. G., Jensen P., 1993, *J. Mol. Spectrosc.*, 161, 219
- Kállay M., Gauss J., 2005, *J. Chem. Phys.*, 123, 214105
- Kállay M., Gauss J., 2008, *J. Chem. Phys.*, 129, 144101
- Kállay M., et al., 2020, *J. Chem. Phys.*, 152, 074107
- Kawashima Y., Suenram R. D., Hirota E., 1996, *J. Mol. Spectrosc.*, 175, 99
- Kendall R. A., Dunning T. H., Harrison R. J., 1992, *J. Chem. Phys.*, 96, 6796
- Kuijpers P., Törring T., Dymanus A., 1975, *Z. Naturforsch. A*, 30
- Kuijpers P., Törring T., Dymanus A., 1976, *Chem. Phys.*, 15, 457
- Lim I. S., Schwerdtfeger P., Metz B., Stoll H., 2005, *J. Chem. Phys.*, 122, 104103
- Matthews D. A., et al., 2020, *J. Chem. Phys.*, 152, 214108
- Miguel Y., Kaltenecker L., Fegley B., Schaefer L., 2011, *ApJ*, 742, L19
- Mitrushchenkov A. O., 2012, *J. Chem. Phys.*, 136, 024108
- Müller H. S. P., Thorwirth S., Roth D. A., Winniewisser G., 2001, *A&A*, 370, L49
- Müller H. S. P., Schlöder F., Stutzki J., Winniewisser G., 2005, *J. Mol. Struct.*, 742, 215
- Neale L., Miller S., Tennyson J., 1996, *ApJ*, 464, 516
- Noumerov B. V., 1924, *MNRAS*, 84, 592
- Owens A., Yachmenev A., Küpper J., Yurchenko S. N., Thiel W., 2018, *Phys. Chem. Chem. Phys.*, 21, 3496
- Owens A., Conway E. K., Tennyson J., Yurchenko S. N., 2020, *MNRAS*, 495, 1927
- Partridge H., Schwenke D. W., 1997, *J. Chem. Phys.*, 106, 4618
- Pearson E. F., Trueblood M. B., 1973, *ApJL*, 179, L145
- Pearson E. F., Winniewisser B. P., Trueblood M. B., 1976, *Z. Naturforsch. A*, 31, 1259
- Pesch P., 1972, *ApJ*, 174, L155
- Peterson K. A., Dunning T. H., 2002, *J. Chem. Phys.*, 117, 10548
- Peterson K. A., Adler T. B., Werner H.-J., 2008, *J. Chem. Phys.*, 128, 084102
- Rajpurohit A. S., Reyle C., Allard F., Homeier D., Schultheis M., Bessell M. S., Robin A. C., 2013, *A&A*, 556, A15
- Raw T. T., Yamamura T., Gillies C. W., 1987, *J. Chem. Phys.*, 87, 3706
- Rivlin T., Lodi L., Yurchenko S. N., Tennyson J., Le Roy R. J., 2015, *MNRAS*, 451, 5153

- Schaefer L., Fegley B., 2009, *ApJ*, 703, L113
- Schaefer L., Lodders K., Fegley Jr. B., 2012, *ApJ*, 755, 41
- Sutcliffe B. T., Tennyson J., 1991, *Int. J. Quantum Chem.*, 39, 183
- Ten-No S., 2004, *Chem. Phys. Lett.*, 398, 56
- Tennyson J., 2012, *WIREs Comput. Mol. Sci.*, 2, 698
- Tennyson J., 2014, *J. Mol. Spectrosc.*, 298, 1
- Tennyson J., 2016, *J. Chem. Phys.*, 145, 120901
- Tennyson J., Sutcliffe B. T., 1986, *Mol. Phys.*, 58, 1067
- Tennyson J., Yurchenko S. N., 2012, *MNRAS*, 425, 21
- Tennyson J., Yurchenko S. N., 2017a, *Mol. Astrophys.*, 8, 1
- Tennyson J., Yurchenko S. N., 2017b, *Int. J. Quantum Chem.*, 117, 92
- Tennyson J., Yurchenko S. N., 2018, *Atoms*, 6, 26
- Tennyson J., Hill C., Yurchenko S. N., 2013, in *6th international conference on atomic and molecular data and their applications ICAMDATA-2012*. AIP, New York, pp 186–195, doi:10.1063/1.4815853
- Tennyson J., et al., 2016, *J. Mol. Spectrosc.*, 327, 73
- Tennyson J., et al., 2020, *J. Quant. Spectrosc. Radiat. Transf.*, 255, 107228
- Tsiaras A., et al., 2016, *ApJ*, 820, 99
- Tsuji T., 1973, *A&A*, 23, 411
- Turner B. E., 1991, *ApJ*, 376, 573
- Tyuterev V. G., Tashkun S. A., Schwenke D. W., 2001, *Chem. Phys. Lett.*, 348, 223
- Watson J. K. G., 2003, *J. Mol. Spectrosc.*, 219, 326
- Weigend F., 2002, *Phys. Chem. Chem. Phys.*, 4, 4285
- Werner H.-J., Knowles P. J., Knizia G., Manby F. R., Schütz M., 2012, *WIREs Comput. Mol. Sci.*, 2, 242
- Werner H.-J., et al., 2020, *J. Chem. Phys.*, 152, 144107
- Yachmenev A., Yurchenko S. N., 2015, *J. Chem. Phys.*, 143, 014105
- Yachmenev A., Yurchenko S. N., Ribeyre T., Thiel W., 2011, *J. Chem. Phys.*, 135, 074302
- Yousaf K. E., Peterson K. A., 2008, *J. Chem. Phys.*, 129, 184108
- Yurchenko S. N., 2014, in , Vol. 10, *Chemical Modelling: Volume 10*. The Royal Society of Chemistry, Chapt. 7, pp 183–228, doi:10.1039/9781849737241-00183
- Yurchenko S. N., Mellor T. M., 2020, *The Journal of Chemical Physics*, 153, 154106
- Yurchenko S. N., Thiel W., Jensen P., 2007, *J. Mol. Spectrosc.*, 245, 126
- Yurchenko S. N., Barber R. J., Yachmenev A., Thiel W., Jensen P., Tennyson J., 2009, *J. Phys. Chem. A*, 113, 11845
- Yurchenko S. N., Yachmenev A., Ovsyannikov R. I., 2017, *J. Chem. Theory Comput.*, 13, 4368
- Yurchenko S. N., Williams H., Leyland P. C., Lodi L., Tennyson J., 2018a, *MNRAS*, 479, 1401
- Yurchenko S. N., Al-Refaie A. F., Tennyson J., 2018b, *A&A*, 614, A131
- Yurchenko S. N., Mellor T. M., Freedman R. S., Tennyson J., 2020, *MNRAS*, 496, 5282
- Zak E. J., Tennyson J., 2017, *J. Chem. Phys.*, 147, 094305
- de Jong W. A., Harrison R. J., Dixon D. A., 2001, *J. Chem. Phys.*, 114, 48
- van Mourik T., Harris G. J., Polyansky O. L., Tennyson J., Császár A. G., Knowles P. J., 2001, *J. Chem. Phys.*, 115, 3706

SUPPORTING INFORMATION

Supplementary data are available at MNRAS online. This includes a detailed description of the methodology, the potential energy and dipole moment surfaces of KOH and NaOH with programs to construct them, and values of the temperature-dependent partition function of KOH and NaOH up to 4000 K. The following references were cited in the supplementary material: (Hill & Peterson 2017; Lim et al. 2005; Peterson & Dunning 2002; Kendall et al. 1992; Werner et al. 2012, 2020; Tyuterev et al. 2001; Partridge & Schwenke 1997; Watson 2003; Jørgensen & Jensen 1993; Owens et al. 2020; Császár et al. 1998; Adler et al. 2007; Peterson et al. 2008; Hill & Peterson 2010; Hill et al. 2009; Ten-No 2004; Yousaf & Peterson 2008; Weigend 2002; Hättig 2005; Yachmenev et al. 2011; Hill et al. 2010; Kállay & Gauss 2005, 2008; Kállay et al. 2020; Matthews et al. 2020; Dunning 1989; Douglas & Kroll 1974; Heß 1986; de Jong et al. 2001; Yurchenko et al. 2007, 2009; Yachmenev & Yurchenko 2015; Tennyson & Yurchenko 2017b; Yurchenko et al. 2017; Yurchenko & Mellor 2020; Carter et al. 1983; Sutcliffe & Tennyson 1991; Noumerov 1924; Cooley 1961; Tennyson & Sutcliffe 1986; Yurchenko et al. 2018b)